



---

**Amphiphilic, phosphonic acid-capped cadmium selenide quantum dots sensitize a thiomolybdate catalyst for hydrogen production**

Journal:	<i>ChemComm</i>
Manuscript ID	CC-COM-07-2024-003656.R1
Article Type:	Communication

SCHOLARONE™  
Manuscripts

## Amphiphilic, phosphonic acid-capped cadmium selenide quantum dots sensitize a thiomolybdate catalyst for hydrogen production

Received 00th January 20xx,  
Accepted 00th January 20xx

Ryan M. Kosko<sup>†a</sup>, Qirui Wang<sup>†a</sup>, Chari Y.M. Peter<sup>a</sup>, Elizabeth O. Phinney<sup>a</sup>, Todd D. Krauss<sup>a,b</sup>, Kara L. Bren<sup>\*a</sup>, Ellen M. Matson<sup>\*a</sup>

DOI: 10.1039/x0xx00000x

**Combining a molecular thiomolybdate cluster,  $[\text{Mo}_3\text{S}_{13}]^{2-}$ , with cadmium selenide quantum dots capped with tetraethyleneglycol monomethyl ether phosphonate (TEGPA) ligands results in a highly active photocatalytic system for the production of hydrogen under visible light irradiation. The system reaches turnover numbers exceeding 30,000 and remains active for ~200 hrs.**

Hydrogen gas ( $\text{H}_2$ ) is an energy-rich fuel that combusts cleanly to generate water and release energy. Currently, most  $\text{H}_2$  is produced industrially through the steam reforming of methane, releasing large amounts of  $\text{CO}_2$ .<sup>1</sup> However, when sourced from water through photolysis or electrolysis,  $\text{H}_2$  presents as a promising carrier of sustainable and renewable energy.<sup>2</sup> This point has motivated a large investment in research activities targeting new approaches for the production of  $\text{H}_2$ .

One class of catalysts that has demonstrated promise in  $\text{H}_2$  evolution are thiomolybdate clusters.<sup>3, 4</sup> These molecular assemblies are truncated forms of nanostructured  $\text{MoS}_2$  that are effective solid-state electrocatalysts for the production of  $\text{H}_2$ .<sup>5, 6</sup> Interest in thiomolybdate cluster catalysts originated from the desire to resolve, with atomic precision, active sites for proton reduction. For a detailed summary of work with these clusters for  $\text{H}_2$  production to date, we refer readers to a recent review published by Streb and Cherevan.<sup>3</sup> Of most relevance to the work presented here are the reports published separately by Streb<sup>7</sup> and Min<sup>8</sup> which describe the use of thiomolybdate clusters in combination with  $\text{Ru}(\text{bpy})_3\text{Cl}_2$  photosensitizers for the photocatalytic reduction of protons. In both reports, high activity for  $\text{H}_2$  evolution was observed. Min and coworkers probe the mechanism of charge transfer between photosensitizer and catalyst, noting that static binding of the components of the photocatalytic system is required for efficient charge transfer.

The work by Streb and Min motivated our interest in employing thiomolybdate clusters as catalysts for proton reduction in combination with cadmium selenide quantum dots (CdSe QDs). Colloidal semiconductor nanocrystal quantum dots are appealing substitutes for molecular photosensitizers, such as  $[\text{Ru}(\text{bpy})_3]^{2+}$ , due to their size-tuneable reduction and oxidation potentials,<sup>9</sup> broad absorption profiles in the visible region,<sup>10</sup> and photostability.<sup>11, 12</sup> These nanocrystals also have high surface areas, which in principle could support association of the thiomolybdate cluster, increasing the probability of occurrence of the static charge transfer events cited as responsible for photocatalytic  $\text{H}_2$  production in the case of the  $\text{Ru}(\text{bpy})_3\text{Cl}_2$ /thiomolybdate system. As such, we hypothesized that pairing CdSe QDs with the thiomolybdate cluster,  $[\text{Mo}_3\text{S}_{13}]^{2-}$ , would yield an active and robust photocatalytic system for proton reduction.

Given the instability of the  $[\text{Mo}_3\text{S}_{13}]^{2-}$  cluster in water,<sup>7</sup> a route to generating colloidally stable CdSe QDs soluble with molar concentrations of polar organic solvents (e.g. acetonitrile, dimethylformamide, dimethylsulfoxide) was required. Traditional CdSe QD syntheses result in the formation of nanocrystals capped with carboxylate ligands with long, greasy, aliphatic hydrocarbons that are incompatible with polar organic solvent.<sup>13-15</sup> Ligand design targeted a phosphonic acid head-group to facilitate ligand exchange from the OA ligands by increasing the binding affinity of the amphiphilic ligand for the surface of the CdSe QD.<sup>16, 17</sup> To confer solubility in polar organic solvent, we opted for a ligand tail derived from repeating glycolate moieties. The compound tetraethylene glycol monomethylether phosphonic acid (TEGPA), originally reported by Jan Ravoo, Glorius and coworkers, meets the aforementioned requirements and has been demonstrated to effectively solubilize metal oxide nanoparticles in polar organic solvent.<sup>18</sup>

Details of the optimized synthesis of TEGPA-capped CdSe QDs (**CdSe-TEGPA**) can be found in the supporting information. Briefly, addition of a methanol solution of TEGPA to a sample of OA-capped CdSe QDs (**CdSe-OA**) suspended in hexane results in complete exchange of the surface ligands. Following work-up, characterization of the **CdSe-TEGPA** was performed via  $^1\text{H}$  NMR and electronic absorption/emission spectroscopies (Figure 1).

<sup>a</sup> Department of Chemistry, University of Rochester, Rochester New York 14627 United States.

<sup>b</sup> Institute of Optics, University of Rochester, Rochester, New York 14627, United States.

<sup>†</sup> Authors contributed equally.

Supplementary Information available: Sample preparation and characterisation, experimental details for photocatalytic  $\text{H}_2$  production,  $\text{H}_2$  generation experiments. See DOI: 10.1039/x0xx00000x

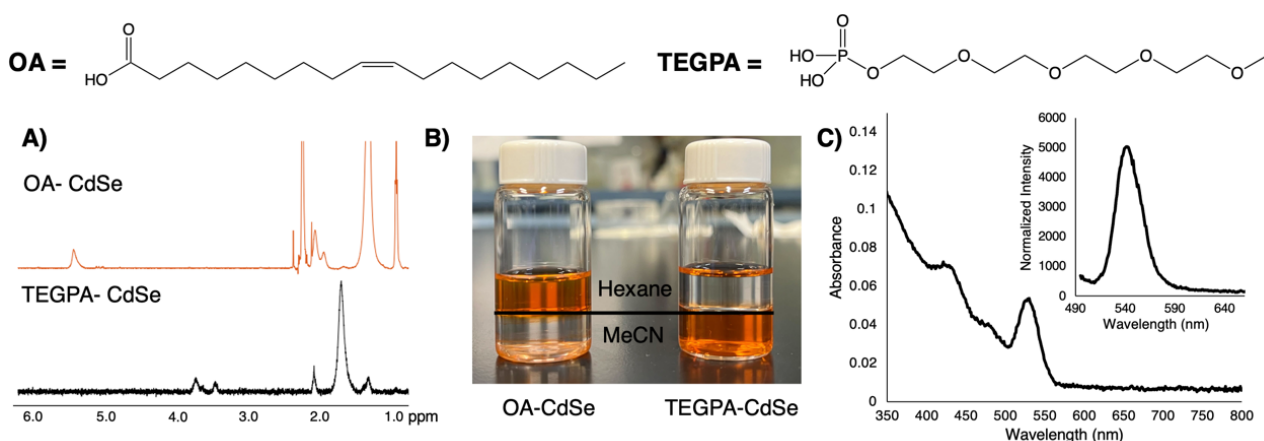


**Figure 1.** Illustration of native OA and TEGPA ligands (top). A)  $^1\text{H}$  NMR spectra of OA-capped CdSe QDs (top, orange) and TEGPA-capped CdSe QDs (bottom, black) collected in  $\text{CDCl}_3$  at  $21^\circ\text{C}$ . B) Image of CdSe QDs depicting change in solubility of nanoparticles; OA-capped QDs are soluble in hexane (top layer, left) while TEGPA-capped QDs are soluble in acetonitrile (bottom layer, right). C) Electronic absorption spectrum and photoluminescence spectrum (inset) of TEGPA-capped CdSe QDs collected in dimethylformamide at room temperature.

The  $^1\text{H}$  NMR spectrum of **CdSe-TEGPA** reveals a loss of the characteristic signal for **CdSe-OA** at  $\sim 5.5$  ppm, suggesting all OA ligands have been removed from the surface of the nanocrystal (Figure 1a). The electronic absorption spectrum of the **CdSe-TEGPA** possesses an absorption feature at 544 nm, shifted from that of the OA-capped CdSe starting material (Figure 1c; Figures S1-S2). Transmission electron microscopy and powder x-ray diffraction of **CdSe-OA** and **CdSe-TEGPA** reveals no substantial changes in the crystal structure or morphology, respectively, of the QDs before and after ligand exchange (Figure S3-S5). Following centrifugation, **CdSe-TEGPA** could be resuspended in a range of polar organic solvents (e.g. MeCN, DMF, DMSO; Figure 1b).

With TEGPA-capped CdSe QDs in hand, we turned our attention to photocatalytic proton reduction. As described in the introduction of this work, our interest was in the investigation of a photocatalytic system using a thiomolybdate catalyst,  $[\text{Mo}_3\text{S}_{13}]^{2-}$ . Initial experiments aimed to mirror the reactivity described for  $[\text{Ru}(\text{bpy})_3]^{2+}$  and  $[\text{Mo}_3\text{S}_{13}]^{2-}$ ; Min and coworkers report optimal catalytic activity in a 9:1 acetonitrile:water mixture (100 mM ascorbic acid).<sup>8</sup> Under these reaction conditions, the **CdSe-TEGPA** and  $[\text{Mo}_3\text{S}_{13}]^{2-}$  produced some  $\text{H}_2$  ( $4.9 \pm 3.3 \mu\text{mol H}_2$ ). However, control experiments performed in the absence of thiomolybdate cluster revealed that the majority of  $\text{H}_2$  was produced by the QDs ( $3.5 \pm 1.9 \mu\text{mol H}_2$ ; Figure S6). Additionally, samples of TEGPA-capped CdSe QDs stored in MeCN become opaque over time ( $\sim 10$  hours), suggesting the nanocrystals have limited colloidal stability in this solvent.

To improve  $\text{H}_2$  production, we evaluated photocatalysis in mixtures of other polar organic solvents (e.g. DMF, DMSO) and water (9:1 ratio as described above; Figure S6). **CdSe-TEGPA** possess enhanced colloidal stability in DMF and DMSO, which we hypothesized would prevent agglomeration of nanoparticles that could lead to the deactivation of the photocatalytic system. While only marginal improvement in proton reduction was observed in mixtures of 9:1 DMSO and water compared to MeCN, we note that the reproducibility

across multiple trials was greatly improved. In contrast, photocatalytic proton reduction experiments performed in 9:1 DMF:water result in significantly improved system activity ( $8.4 \pm 0.9 \mu\text{mol}$ ; Figures 2 and S6-S7). Control experiments investigating the activity of the **CdSe-TEGPA** for proton reduction under analogous conditions in the absence of thiomolybdate cluster revealed no production of  $\text{H}_2$  (Figure S8). Similarly, the clusters are inactive for photocatalytic  $\text{H}^+$  reduction in the absence of **CdSe-TEGPA** (Figure S8). The activity of  $[\text{Ru}(\text{bpy})_3]^{2+}$  and  $[\text{Mo}_3\text{S}_{13}]^{2-}$  in DMF:water mixtures (9:1, 100 mM ascorbic acid) is poor ( $0.25 \pm 0.05 \mu\text{mol H}_2$ ); this result is consistent with previous reports,<sup>8</sup> and is attributed to poor ion pairing interactions between the cluster and photosensitizer in DMF.

In DMF:water mixtures, photocatalytic systems utilizing **CdSe-TEGPA** as a photosensitizer for  $[\text{Mo}_3\text{S}_{13}]^{2-}$  outperform systems using  $[\text{Ru}(\text{bpy})_3]^{2+}$ . However, the total activity of the QD/thiomolybdate photocatalytic system, as measured in turnover number ( $\text{TON} = 170 \pm 20 \text{H}_2$ ), does not reach levels previously reported with  $[\text{Ru}(\text{bpy})_3]^{2+}$  ( $\text{TON} = 1500$ ).<sup>8</sup> In order to

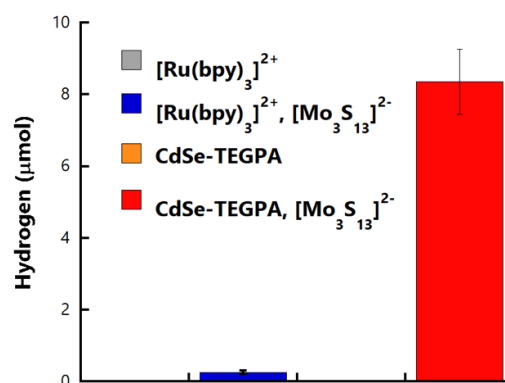


**Figure 2.** Total  $\text{H}_2$  production after 24 hr (530-nm LEDs; 12 mW),  $10 \mu\text{M}$   $[\text{Mo}_3\text{S}_{13}]^{2-}$  and 100 mM ascorbic acid in 9:1 DMF:water mixtures using  $1 \mu\text{M}$  **CdSe-TEGPA** or  $100 \mu\text{M}$   $[\text{Ru}(\text{bpy})_3]^{2+}$  as a photosensitizer. All reactions were shaken at 100 rpm and held at  $31^\circ\text{C}$ .

improve the performance of the **CdSe-TEGPA**/[**Mo<sub>3</sub>S<sub>13</sub>**]<sup>2-</sup> photocatalytic system, we sought to understand which components limit activity by replenishing photosensitizer, catalyst and/or electron donor after system activity plateaus (Figure S7). While single component replenishment experiments performed after 24 hrs had little effect (< 20% initial activity recovered), addition of both **CdSe-TEGPA** and ascorbic acid together to “spent” mixtures results in the restoration of 56% activity (Figure S9). This observation suggests that the catalyst remains functional following photocatalysis, indicating that system activity is limited by availability of the electron donor and stability of the photosensitizer.

With this knowledge, we attempted to increase the concentration of ascorbic acid in our system. However, the maximum solubility of ascorbic acid in 9:1 DMF:water is ~200 mM; when higher concentrations were employed, white crystalline precipitate was observed that complicates light absorption and photocatalysis. To increase the concentration of ascorbic acid without compromising the homogeneity of the system, we explored the consequences of increasing the molar ratio of water in our experiments (Figure 3). We tested solvent ratios of DMF:water of 9:1 to 1:9 with 200 mM ascorbic acid per equivalent of water (the maximum solubility for the 9:1 ratio; Figure 3a). To our surprise, we observed a large increase in H<sub>2</sub> production, with optimal activity in 6:4 DMF:water ratios with 800 mM ascorbic acid (371.1 ± 12.3 μmol H<sub>2</sub>). At higher equivalents of water and increased ascorbic acid concentration, activity rolled over. This observation is consistent with the instability of **CdSe-TEGPA** in water over prolonged periods of time, as well as the reported deactivation of the thiomolybdate catalyst in water through ligand substitution reactions.<sup>7</sup>

In order to deconvolute the effects of ascorbic acid and water fraction in the reaction mixture, we evaluated different concentrations of ascorbic acid in a 6:4 ratio of DMF:water. When the concentration of ascorbic acid was increased from 200 mM to 800 mM, we observed optimal activity at 800 mM ascorbic acid (Figure S10, Table 1). Interestingly, with 200 mM ascorbic acid in DMF:water (6:4 ratio) we observed greater H<sub>2</sub> production (58.1 ± 4.9 μmol H<sub>2</sub>) than that observed in DMF:water (9:1 ratio) with 200 mM ascorbic acid (18.4 ± 3.9 μmol; Table 1.) This suggests that both the fraction of water and availability of ascorbic acid play a role in increasing the amount of H<sub>2</sub> produced.

Finally, experiments were performed in an attempt to optimize TON and longevity of the photocatalytic system (Table 1). We employed [**Mo<sub>3</sub>S<sub>13</sub>**]<sup>2-</sup> in concentrations ranging from 1 μM to 10 μM (Figure S11, Table 1). We found that the overall magnitude of H<sub>2</sub> produced increases with increasing catalyst concentration, but optimal TONs are observed with low (1 μM) concentration of catalyst (51.7 ± 11.4 μmol H<sub>2</sub>, 10300 ± 2200 TON with respect to [**Mo<sub>3</sub>S<sub>13</sub>**]<sup>2-</sup>). Using the system optimized for TON, we next evaluated the longevity of the system. We found that catalysis continues for about 200 hrs before production of H<sub>2</sub> plateaus, reaching maximum TONs of 27300 ± 8500 (Figure 3B). The system using **CdSe-TEGPA** shows incredibly high activity and longevity that outcompetes previous reports of

homogenous photochemical H<sub>2</sub> evolution with [**Mo<sub>3</sub>S<sub>13</sub>**]<sup>2-</sup> and [Ru(bpy)<sub>3</sub>]<sup>2+</sup>, employing modest concentrations of catalyst and much lower concentrations of **CdSe-TEGPA** photosensitizer.<sup>8</sup>

Next, experiments were performed to determine whether [**Mo<sub>3</sub>S<sub>13</sub>**]<sup>2-</sup> binds to the surface of the **CdSe-TEGPA** QDs during photocatalysis. Following irradiation for 30 hrs, we observe that QDs precipitate. The pellet and supernatant were then separated for further analysis. Fresh solution (DMF:water 6:4) containing 200 mM ascorbic acid was added to the pellet and the system was irradiated for a further 76 hrs. The redispersion of the pellet resulted in 27.6 ± 10.3 μmol of H<sub>2</sub>. The addition of fresh **CdSe-TEGPA** to the supernatant resulted in 3.6 ± 0.5 μmol of H<sub>2</sub> over the same period (Figure S12). The enhanced H<sub>2</sub> production with the redispersed QD pellet suggests [**Mo<sub>3</sub>S<sub>13</sub>**]<sup>2-</sup> is associated with the pellet.

To further demonstrate thiomolybdate cluster association with the QD surface we performed inductively coupled plasma-mass spectrometry (ICP-MS). Analysis of the pellet and supernatant reveals that 86% of the Mo is present in the pellet, agreeing with our observations from photocatalysis (Table S1).

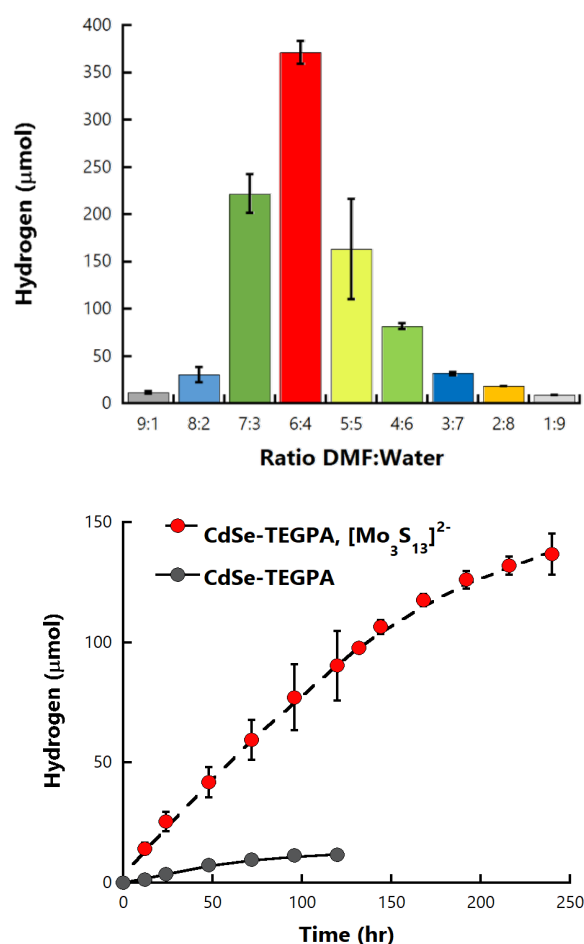


**Figure 3. (top)** Photochemical H<sub>2</sub> evolution (48 hr) with **CdSe-TEGPA** (1.0 μM), [**Mo<sub>3</sub>S<sub>13</sub>**]<sup>2-</sup> (10 μM) and ascorbic acid (200-1000 mM) in DMF:water (ratio shown in figure). Experiments contained 200 mM ascorbic acid per equivalent of water. 530 nm LED irradiation, 31 °C, 100 rpm. **(bottom)** Time course photochemical H<sub>2</sub> evolution with **CdSe-TEGPA** (1.0 μM), [**Mo<sub>3</sub>S<sub>13</sub>**]<sup>2-</sup> (1.0 μM) and ascorbic acid (800 mM) in DMF:water (6:4). 530-nm LED irradiation, 31 °C, 100 rpm.

**Table 1.** Overview of experiments performed to optimize H<sub>2</sub> production with CdSe-TEGPA/[Mo<sub>3</sub>S<sub>13</sub>]<sup>2-</sup> photochemical systems. TONs are reported with respect to catalyst, [Mo<sub>3</sub>S<sub>13</sub>]<sup>2-</sup>. All experiments used 1.0 μM CdSe-TEGPA.

[Catalyst] (μM)	[AA] <sup>a</sup> (mM)	DMF:Water Ratio	TON (Longevity)
10.0	100	9:1	170 ± 20 (24 hr)
10.0	200	9:1	370 ± 80 (24 hr)
10.0	200	6:4	1200 ± 100 (48 hr)
10.0	400	6:4	2200 ± 200 (48 hr)
10.0	600	6:4	4600 ± 100 (48 hr)
10.0	800	6:4	6700 ± 100 (48 hr) 10900 ± 900 (168 hr)
1.0	800	6:4	10300 ± 2300 (48 hr) 27300 ± 8500 (240 hr)
2.0	800	6:4	7900 ± 200 (48 hr)
5.0	800	6:4	7100 ± 50 (48 hr)
10.0	800	6:4	5000 ± 550 (48 hr)

<sup>a</sup> AA = ascorbic acid (sacrificial electron donor, source of protons).

The improved activity of the system compared to [Ru(bpy)<sub>3</sub>]<sup>2+</sup> is attributed to the binding of [Mo<sub>3</sub>S<sub>13</sub>]<sup>2-</sup> and CdSe-TEGPA.<sup>17, 19</sup>

The photocatalytic system reported here capitalizes on the use of TEGPA capping ligands that render the semiconducting nanocrystals soluble in a range of polar organic solvents. This result establishes a new class of photosensitizer for the small molecule activation reactions. With relevance to this work, CdSe-TEGPA has low background proton reduction activity in DMF:water mixtures, making these systems potential photosensitizers for the *selective* reduction of other small molecule substrates; this is the subject of ongoing investigations by our research team. Here, we demonstrate that when CdSe-TEGPA is paired with the thiomolybdate cluster, [Mo<sub>3</sub>S<sub>13</sub>]<sup>2-</sup>, a highly active photocatalytic system for H<sub>2</sub> production is achieved. In comparison to prior reports that use [Ru(bpy)<sub>3</sub>]<sup>2+</sup> as a photosensitizer for H<sub>2</sub> production with the same thiomolybdate cluster as the catalyst, CdSe-TEGPA/[Mo<sub>3</sub>S<sub>13</sub>]<sup>2-</sup> combinations achieve higher TONs and longevity, (~200 hr vs. 24 hr).

This work is supported by the Chemical Sciences, Geosciences, and Biosciences Division, Office of Basic Energy Sciences, Office of Science, U.S. Department of Energy, Grant No. DE-SC002106. The authors acknowledge William W. Brennessel from the University of Rochester for his assistance in collecting the powder X-ray diffraction data. The authors acknowledge Thomas Scrimale M.S. for his assistance with collecting ICP-MS data and Dr. Sean O'Neill for his assistance with collecting TEM images.

## Conflicts of interest

There are no conflicts to declare.

## Data availability

The data that supports the findings of this study are available in the manuscript and ESI of this article.

## References

1. A. Boretti and B. K. Banik, *Adv. Energy and Sustainability Res.*, 2021, **2**, 2100097.
2. K. C. Christoforidis and P. Fornasiero, *ChemCatChem*, 2017, **9**, 1523-1544.
3. S. Batool, M. Langer, S. N. Myakala, M. Heiland, D. Eder, C. Streb and A. Cherevan, *Adv. Mater.*, 2024, **36**, 2305730.
4. M.-L. Grutza, A. Rajagopal, C. Streb and P. Kurz, *Sustainable Energy Fuels*, 2018, **2**, 1893-1904.
5. T. F. Jaramillo, K. P. Jørgensen, J. Bonde, J. H. Nielsen, S. Horch and I. Chorkendorff, *Science*, 2007, **317**, 100-102.
6. B. Hinnemann, P. G. Moses, J. Bonde, K. P. Jørgensen, J. H. Nielsen, S. Horch, I. Chorkendorff and J. K. Nørskov, *J. Am. Chem. Soc.*, 2005, **127**, 5308-5309.
7. M. Dave, A. Rajagopal, M. Damm-Ruttensperger, B. Schwarz, F. Nägele, L. Daccache, D. Fantauzzi, T. Jacob and C. Streb, *Sustainable Energy Fuels*, 2018, **2**, 1020-1026.
8. Y. Lei, M. Yang, J. Hou, F. Wang, E. Cui, C. Kong and S. Min, *Chem. Commun.*, 2018, **54**, 603-606.
9. J. Jasieniak, M. Califano and S. E. Watkins, *ACS Nano*, 2011, **5**, 5888-5902.
10. A. P. Alivisatos, *J. Phys. Chem.*, 1996, **100**, 13226-13239.
11. M. Bruchez, M. Moronne, P. Gin, S. Weiss and A. P. Alivisatos, *Science*, 1998, **281**, 2013-2016.
12. Z. Han, F. Qiu, R. Eisenberg, P. L. Holland and T. D. Krauss, *Science*, 2012, **338**, 1321-1324.
13. S. Flamee, M. Cirillo, S. Abe, K. De Nolf, R. Gomes, T. Aubert and Z. Hens, *Chem. Mater.*, 2013, **25**, 2476-2483.
14. Y. Yin and A. P. Alivisatos, *Nature*, 2005, **437**, 664-670.
15. M. B. Mohamed, D. Tonti, A. Al-Salman, A. Chemseddine and M. Chergui, *J. Phys. Chem. B*, 2005, **109**, 10533-10537.
16. R. Gomes, A. Hassinen, A. Szczygiel, Q. Zhao, A. Vantomme, J. C. Martins and Z. Hens, *J. Phys. Chem. Lett.* 2011, **2**, 145-152.
17. R. R. Knauf, J. C. Lennox and J. L. Dempsey, *Chem. Mater.*, 2016, **28**, 4762-4770.
18. N. Möller, A. Rühling, S. Lamping, T. Hellwig, C. Fallnich, B. J. Ravoo and F. Glorius, *Angew. Chem. Int. Ed.*, 2017, **56**, 4356-4360.
19. Jeong, S.; Achermann, M.; Nanda, J. Ivanov, S.; Klimov, V.I.; Hollingsworth, J.A. *J. Am. Chem. Soc.* 2006, **127**, 10126-10127.

Data Availability Statement for Manuscript Entitled: **Amphiphilic, phosphonic acid-capped cadmium selenide quantum dots sensitize a thiomolybdate catalyst for hydrogen production**

The data that supports the findings of this study are available in the manuscript and electronic supporting information (ESI) of this article.